Available online at www.sciencedirect.com
ScienceDirect
Journal of Sound and Vibration 311 (2008) 1409–1419
JOURNAL OF SOUND AND VIBRATION
www.elsevier.com/locate/jsvi

Short Communication

An experimental investigation of nonlinear vibration and frequency response analysis of cantilever viscoelastic beams

S. Nima Mahmoodi[a], Nader Jalili[a,*], Siamak E. Khadem[b]

[a]*Smart Structures and Nanoelectromechanical Systems Laboratory, Department of Mechanical Engineering, Clemson University, Clemson, SC 29634-0921, USA*

[b]*Department of Mechanical Engineering, School of Engineering, Tarbiat Modarres University, P.O. Box 14115-177, Tehran, Iran*

Received 18 May 2006; received in revised form 13 September 2007; accepted 20 September 2007
Available online 29 October 2007

Abstract

The nonlinear vibration analysis of a directly excited cantilever beam modeled as an inextensible viscoelastic Euler–Bernoulli beam has been studied by the authors and is reported in the literature. The viscoelastic damping was modeled as Kelvin–Voigt damping, and the nonlinearities arisen from the inextensibility assumption. This paper extends our theoretical developments presented in the previous papers and utilizes the method of multiple scales in order to arrive at the modulation equations and the closed-form frequency response function. The analytically derived frequency response is experimentally verified through harmonic force excitation of samples of carbon nanotube-reinforced beams. The beam used in experiment consists of two elastic layers of high-carbon steel sandwiched together through a viscoelastic layer of carbon nanotube–epoxy mixture. The results demonstrate that increasing the excitation amplitude or decreasing damping ratio can cause a minor decrease in the nonlinear resonance frequency despite the significant increase in the amplitude of vibration due to reduced damping.

1. Introduction

The nonlinear vibrations of directly excited viscoelastic beam have been studied analytically [1,2]. The beam was assumed to be inextensible and followed a classical linear viscoelastic behavior, i.e., Kelvin–Voigt model. There are other studies on dynamical modeling of viscoelastic beams, where analytical models for sandwiched beams have been proposed and investigated by several researchers ([3,4] are just a few examples). The Kelvin–Voigt model is utilized here as the viscoelastic model of the beam. This model has been used to study the vibration damping of nonlinear viscoelastic systems [5] and analysis of nonlinear oscillations of simply supported viscoelastic rectangular plates [6]. Knowing the geometry and viscoelastic model of the system, the equations of motion are obtained considering the direct forced bending vibrations of the system.

In Ref. [1], an Euler–Bernoulli beam model for a long and thin viscoelastic beam structure was assumed. A geometrical approach was utilized to study the bending vibrations of such viscoelastic system. The beam

*Corresponding author. Tel.: +1 864 656 5642.
E-mail address: jalili@clemson.edu (N. Jalili).

0022-460X/$ - see front matter © 2007 Elsevier Ltd. All rights reserved.
doi:10.1016/j.jsv.2007.09.027

was considered to be inextensible and only planar vibration was considered. Such a model has been used by several researchers [7–14]. The planar and nonplanar nonlinear vibrations of elastic beams have been studied earlier [15,16]. In these systems, the geometry of the system causes the presence of nonlinear terms in inertia, damping and stiffness. In nonlinear vibrations of elastic beams, mainly nonlinearities of inertia and stiffness exist while damping nonlinearity is negligible [17,18]. Other nonlinearities are produced due to presence of friction and structural damping [19]. These two nonlinear terms are nonlinearities in damping.

Although there are many numerical methods such as finite element methods [20] to analyze the nonlinear vibration of flexible beams, an analytical method, i.e., method of multiple scales, is utilized in Ref. [1] to derive a closed-form solution for the nonlinear frequency equations. This method has been used for the analysis of nonlinear vibrations of damped and undamped systems, and nonlinear nonplanar oscillations of elastic cantilever beams excited by a combination of parametric resonance in which the effect of geometric and inertial nonlinearities in the governing equations of motion and boundary conditions are considered [19,21]. Analytical study conducted here concludes a relationship for the modulation equations and frequency response function, and hence, amplitude-dependent nonlinear frequencies can result. The closed-form solution helps better understand the dependence of the system to its physical and geometrical parameters and can be used for control of the system [22]. In addition, the proposed method has already been used to derive the closed-form solution of nonlinear vibration problems with nonlinear terms of damping and stiffness [23].

In this paper, using the equations of motion of the planar bending vibration of an inextensible viscoelastic carbon nanotubes-reinforced cantilever beam, the stability of the system is analytically studied and experimentally verified. The motivation behind utilization of carbon nanotubes-reinforced beam in this study originates from their interesting properties including damping enhancement [24,25]. Carbon nanotubes have also other astounding properties such as very high elastic modulus and high electric current capacity when compared with other conductive materials [24–26]. The rest of the paper is organized as follows. In the immediately following section, the modeling assumptions and frequency response analysis using the method of multiple scales are presented. Experimental setup and results are provided in Sections 3 and 4, and finally Section 5 concludes the research and provides future works.

2. Nonlinear frequency response

In the derivation of the equations of motions and stability analysis of the nonlinear vibration of the viscoelastic beam considered here, the boundary conditions are considered to be clamped–free (see Fig. 1). The beam is assumed to be inextensible and a classical linear viscoelastic model, i.e. Kelvin–Voigt model is considered. It is assumed that the beam follows the Euler–Bernoulli beam theory, where shear deformation and rotary inertia terms are negligible. The beam is also assumed to possess uniform cross-sectional area. The non-dimensional form of equations of motion and boundary conditions of the beam, shown in Fig. 1,

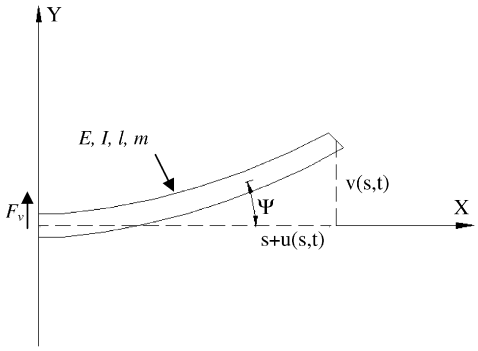

Fig. 1. Schematic of the cantilever beam.

can be obtained as [1,2]

$$\ddot{v}+\varepsilon\eta\dot{v}^{\mathrm{iv}}+v^{\mathrm{iv}}+\frac{1}{2}\varepsilon\left[v'\int_1^x\int_0^x\left(\dot{v}'^2+v'v\ddot{v}'\right)\mathrm{d}x\,\mathrm{d}x\right]'+\varepsilon[v'(v'v'')']'+\frac{1}{2}\varepsilon\eta\frac{\partial}{\partial t}\left[v''v'^2\right]''+f\cos(\Omega t)=0, \tag{1}$$

$$v=v'=0\quad\text{at } x=0\quad\text{and}\quad v''=v'''=0\quad\text{at } x=1, \tag{2}$$

where v is the bending vibration, η the strain-rate damping coefficient (which appears due to Kelvin–Voigt model), Ω the excitation frequency, and ε the perturbation parameter (in order to use the method of multiple scales [27,28]). The beam bending vibration, v, can be expanded by order of ε as

$$v(x,t;\varepsilon)=v_0(x,T_0,T_1)+\varepsilon v_1(x,T_0,T_1)+\cdots, \tag{3}$$

where T_0 and T_1 are the time scales. $T_1=\varepsilon t$ is a slow time scale, demonstrating shift in the natural frequencies because of the nonlinearity, while $T_0=t$ acts as a fast time scale, characterizing motions occurring at the natural frequencies, ω_k.

Substituting expression (3) into the partial differential equations of system (1) and boundary conditions (2) and separating terms at orders of ε, yields

$$(\varepsilon^0):\frac{\partial^2 v_0}{\partial T_0^2}+v_0^{\mathrm{iv}}=0, \tag{4}$$

$$v_0=v_0'=0\quad\text{at } x=0\quad\text{and}\quad v_0''=v_0'''=0\text{ at } x=1, \tag{5}$$

$$\begin{aligned}(\varepsilon^1):\frac{\partial^2 v_1}{\partial T_0^2}+v_1^{\mathrm{iv}}=&-2\frac{\partial^2 v_0}{\partial T_0\,\partial T_1}-\eta\frac{\partial v_0^{\mathrm{iv}}}{\partial T_0}-\frac{1}{2}\left[v_0'\int_1^s\int_0^s\left(\frac{\partial \dot{v}_0'^2}{\partial T_0}+v_0'\frac{\partial^2 v_0'}{\partial T_0^2}\right)\mathrm{d}x\,\mathrm{d}x\right]'-[v_0'(v_0'v_0'')']'\\&-\eta\left[\frac{1}{2}\frac{\partial \dot{v}_0''}{\partial T_0}v_0'^2+v_0''v_0'\frac{\partial \dot{v}_0'}{\partial T_0}\right]''+f\cos(\Omega T_0),\end{aligned} \tag{6}$$

$$v_1=v_1'=0\quad\text{at } x=0\quad\text{and}\quad v_1''=v_1'''=0\text{ at } x=1. \tag{7}$$

The Galerkin approximation can now be used to represent $v(x,t)$ as a series of products of spatial functions of only x and time-dependent functions as

$$v(x,t)=\sum_{n=1}^{\infty}v_n(x,t)=\sum_{n=1}^{\infty}p_n(x)q_n(t), \tag{8}$$

where p_n are the eigenfunctions of a linear uniform cantilever beam and q_n are the generalized time-dependent coordinates. The solution of linear equation (4) with the boundary conditions (5) can be given as

$$v_0=\tfrac{1}{2}p_k(x)\left[a_k(T_1)\mathrm{e}^{\mathrm{i}\beta_k(T_1)}\mathrm{e}^{\mathrm{i}\omega_k T_0}+a_k(T_1)\mathrm{e}^{-\mathrm{i}\beta_k(T_1)}\mathrm{e}^{-\mathrm{i}\omega_k T_0}\right], \tag{9}$$

where a_k and β_k can be found by applying the solvability conditions to the problem as discussed later in this section. The solvability condition demands that the eigenfunctions be orthogonal, i.e.

$$\langle p_n(x),p_m(x)\rangle=\int_0^1 p_n(s)p_m(s)\,\mathrm{d}s=\delta_{nm} \tag{10}$$

and δ_{nm} is the Kronecker delta. For the case of primary resonance,

$$\Omega=\omega_k(1+\varepsilon\sigma), \tag{11}$$

where σ is the detuning parameter. Substituting Eqs. (9) and (11) into (6), and applying the condition of Eq. (10), the secular terms which should be equal to zero become

$$2\mathrm{i}\omega_k\left(\frac{1}{2}a_k'+\frac{1}{2}\mathrm{i}a_k\beta_k'\right)+\frac{1}{2}\mathrm{i}\eta\omega_k a_k+(3\alpha_1-2\alpha_2\omega_k^2+\mathrm{i}\omega_k\alpha_4)\frac{a_k^3}{8}-F_k\mathrm{e}^{\mathrm{i}(\omega_k\sigma T_1-\beta_k)}=0, \tag{12}$$

where

$$F_k = \int_0^1 \frac{f}{2} p_k(x)\,\mathrm{d}x, \tag{13}$$

$$\alpha_1(\omega_k) = \langle p_k(x),\ [p_k'(p_k'p_k'')]' \rangle, \tag{14}$$

$$\alpha_2(\omega_k) = \left\langle p_k(x), \left[p_k' \int_1^x \int_0^x {p_k'}^2\,\mathrm{d}x\,\mathrm{d}x \right] \right\rangle \tag{15}$$

and

$$\alpha_4(\omega_k) = \left\langle p_k(x), \eta \left[3{p_k'}^2 p_k'' \right]'' \right\rangle. \tag{16}$$

Separating the real and imaginary parts of Eq. (12) in the form of

$$a_k' = -\frac{1}{2}\eta a_k - \alpha_4 \frac{a_k^3}{8} + \frac{F_k}{\omega_k}\sin(\omega_k \sigma T_1 - \beta_k), \tag{17}$$

$$a_k \beta_k' = \left(3\alpha_1 - 2\alpha_2\omega_k^2\right)\frac{a_k^3}{8\omega_k} - \frac{F_k}{\omega_k}\cos(\omega_k \sigma T_1 - \beta_k) \tag{18}$$

defining γ as a new phase parameter

$$\gamma_k = \omega_k \sigma T_1 - \beta_k \tag{19}$$

and substituting Eq. (19) into (17) and (18), the modulation equations can be obtained as

$$a_k' = -\frac{1}{2}\eta a_k - \alpha_4 \frac{a_k^3}{8} + \frac{F_k}{\omega_k}\sin(\gamma_k), \tag{20}$$

$$a_k \gamma_k' = \omega_k \sigma a_k - (3\alpha_1 - 2\alpha_2\omega_k^2)\frac{a_k^3}{8\omega_k} + \frac{F_k}{\omega_k}\cos(\gamma_k). \tag{21}$$

Using modulation equations, the frequency response of the system reduces to

$$\left(\frac{1}{2}\eta a_k + \alpha_4 \frac{a_k^3}{8}\right)^2 + \left(\omega_k \sigma a_k - \left(3\alpha_1 - 2\alpha_2\omega_k^2\right)\frac{a_k^3}{8\omega_k}\right)^2 = \left(\frac{F_k}{\omega_k}\right)^2. \tag{22}$$

Solving the frequency response function (22) for σ results in

$$\sigma_1 = (3\alpha_1 - 2\alpha_2\omega_k^2)\frac{a_k^2}{8\omega_k^2} + \frac{1}{a_k\omega_k}\sqrt{\left(\frac{F_k}{\omega_k}\right)^2 - \left(\frac{1}{2}\eta a_k + \alpha_4 \frac{a_k^3}{8}\right)^2}, \tag{23}$$

$$\sigma_2 = (3\alpha_1 - 2\alpha_2\omega_k^2)\frac{a_k^2}{8\omega_k^2} - \frac{1}{a_k\omega_k}\sqrt{\left(\frac{F_k}{\omega_k}\right)^2 - \left(\frac{1}{2}\eta a_k + \alpha_4 \frac{a_k^3}{8}\right)^2}. \tag{24}$$

Using the modeling efforts developed here, the vibration of the viscoelastic beam can be numerically illustrated. Considering the beam in Fig. 1 with the physical properties listed in Table 1, the frequency response of the system due to a direct excitation of the first mode may be obtained as shown in Fig. 2.

In the following section, the frequency response function developed here is experimentally verified. A comparison study will follow to verify the modeling assumptions taken here.

3. Experimental setup and methods

The experimental investigation of the nonlinear vibrations of the beam system is presented here when considering its first mode. This section provides the process of fabricating the beam followed by the experimental setup and results as discussed next.

Table 1
Physical properties of the viscoelastic cantilever beam

Symbol	Property	Value
EI	Beam rigidity	0.453 Pa m^4
l	Beam length	140 mm
w_b	Beam width	12.5 mm
h_1	Viscoelastic layer thickness	1.25 mm
h_2	Steel layer thickness (each)	0.86 mm

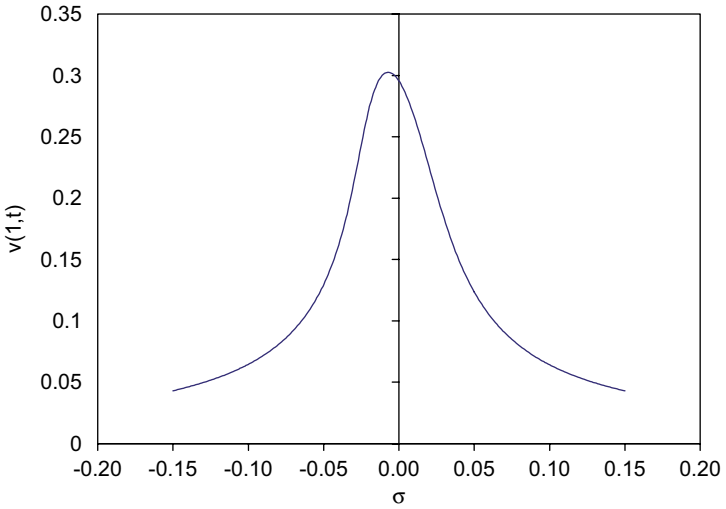

Fig. 2. Frequency response curve for damping ratio $\eta = 0.063$ and force $f = 0.08$ N.

3.1. Fabrication of the viscoelastic beam

The viscoelastic beam considered here consists of three layers, as shown in Fig. 3. The two outer elastic layers are high-carbon steel with elastic modulus of 190 GPa. In order to make the viscoelastic layer, 1 g of epoxy resin and 1 g of epoxy hardener are mixed, and depending on the sample, 0%, 2.5% or 5% (percentages are by weight) multiwalled carbon nanotube (MWCNT) is added and mixed with the resin. The carbon nanotube is added on one side of both steel layers and then sandwiched to form a viscoelastic layer between the two steel layers. The viscoelastic beam is then cured at room temperature for about 5 h under a load of 20 N. Following this, the samples were cured at 60 °C for about 24 h under no load. Finally, the beam was brought to room temperature and the extra resin coming out of the edges was trimmed and the beams were cleaned [25]. As reported in Ref. [25], the equivalent damping ratio η for the samples were found to be $\eta = 0.08$ for 2.5% MWCNT and $\eta = 0.063$ for 5% MWCNT.

3.2. Experimental setup

The beam fabricated in the previous subsection is now subjected to a harmonic force excitation over the length of the beam. In order to experimentally simulate this condition, one end of the beam is mounted to an inertial actuator via an impedance head. The impedance head is used to simultaneously provide base acceleration and excitation force measurements. A laser sensor is also utilized to measure the vibrations of the tip of the beam. The setup is shown in Fig. 4.

As explained earlier, a layer of MWCNT mixed with epoxy is sandwiched between two high-carbon steel layers with the thickness of 0.86 mm each. A closer picture of the beam is depicted in Fig. 5. The beam

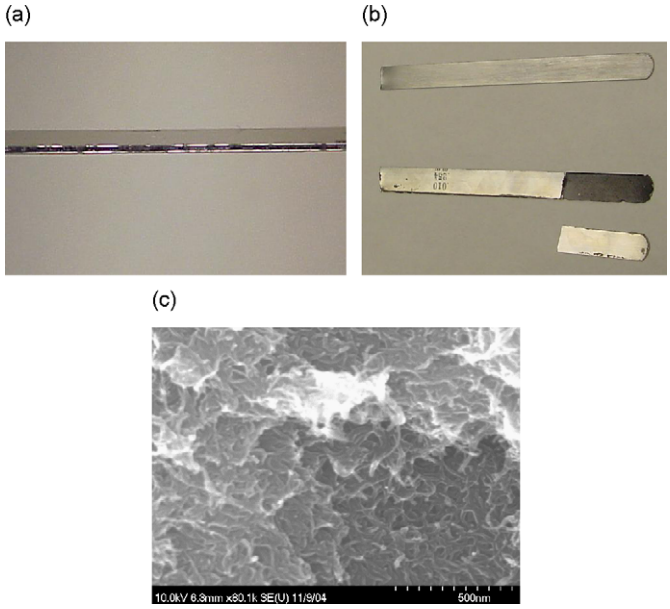

Fig. 3. (a) A schematic of a MWCNT-reinforced beam, (b) different beam layers and (c) scanning electron microscopy (SEM) image of the multiwalled MWCNT–epoxy composite.

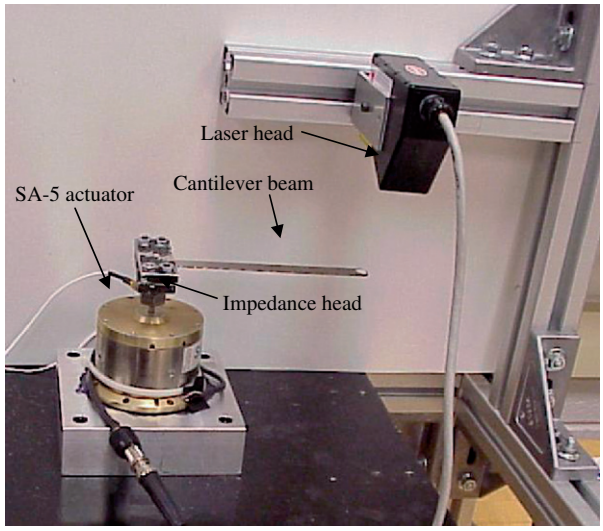

Fig. 4. Experimental setup for the beam with base excitation.

length is 140 mm with its width of about 12.5 mm. There are three samples with different viscoelastic layers, namely; a plain epoxy layer, 2.5% MWCNT mixed with epoxy, and finally 5% MWCNT mixed with epoxy.

To excite the viscoelastic beam, an electromagnetic inertial actuator (SA-5) is used, as shown in Fig. 4. On top of the shaker, a PCB model 288D01 impedance head sensor connects the shaker to the structure where beam is clamped in. The impedance head provides measurements for both the base acceleration and excitation force. The vibration of the tip is measured and monitored by a DynaVision LDS laser distance sensor. All signals are sent and processed via a dSPACE® CP1104 board, which is utilized by ControlDesk® and Matlab Simulink® software packages.

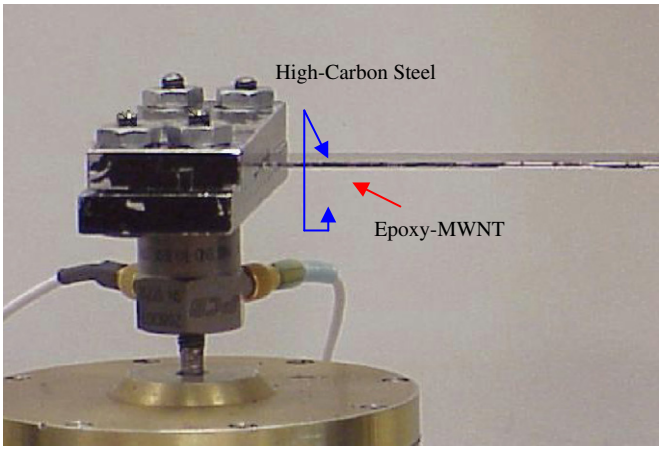

Fig. 5. Arrangement of the MWCNT-reinforced viscoelastic beam clamped to an inertial actuator.

3.3. Test method and configurations

Three beams with different viscoelastic layers (plain epoxy, 2.5% MWCNT mixed with epoxy and 5% MWCNT mixed with epoxy) are utilized for the tests. For each beam, four experimental runs are performed. In the first three runs, the beam is excited with a harmonic force with constant amplitude and excitation frequency near the first mode of the beam. A frequency sweep is performed and the amplitude is measured near natural frequency. In the second and third runs, the amplitude of excitation changes to another constant value and again the frequency is swept. In the fourth run, the beam is excited in its first vibrational mode and then the excitation is removed and the vibration is measured in order to study the damping effects.

In the first three runs, the frequency is swept from -20% of the first natural frequency to 20% over it, and the vibration amplitude is measured and recorded. The frequency sweep has been done in both directions of low to high and high to low frequencies. Through extensive runs, it is found that the first vibration mode for the plain (0% MWCNT) epoxy is about 22 Hz, 2.5% MWCNT–epoxy is about 33.5 Hz, and 5% MWCNT–epoxy is about 37 Hz. In the second run, the amplitude of excitation is decreased to 0.6 (and 0.3 for the third run) of the amplitude of the first run (with its amplitude being 1) and the same process of the first run was performed. In the forth run, the beams were excited at their first natural frequencies with amplitude of 0.15 of the first run, the excitation is then removed and vibration amplitude is measured. The sampling frequency rate is 0.5 Hz. In each step after shifting to new excitation frequency, it is waited enough for the response to become steady and then the amplitude is measured.

The actual position of the laser is about 2–4 mm above the tip of the beam. However, it is considered that the laser position is the tip in numerical calculations. This means if the beam length is considered to be $x = 1.0$, then the position of the laser is at $x = 0.97$. A more closer observation on Fig. 3b, it is seen that the tip of the beam is rounded so the mass per length at the tip is less than the rest of the beam. These two conditions bring small errors in calculations of natural frequency. However, by numerically studying these conditions and their error effects on the analysis, it appears that they compensate and the combined error is negligible.

4. Results and discussions

The equations of motion of the carbon nanotube-reinforced beam have been derived, and using the method of multiple scales a closed-form solution has been presented. Considering the properties of the beams used in the experiment (see Table 1), the frequency response function of the beams has been plotted using the mathematical model derived in Section 2. These results can now be experimentally verified. The frequency

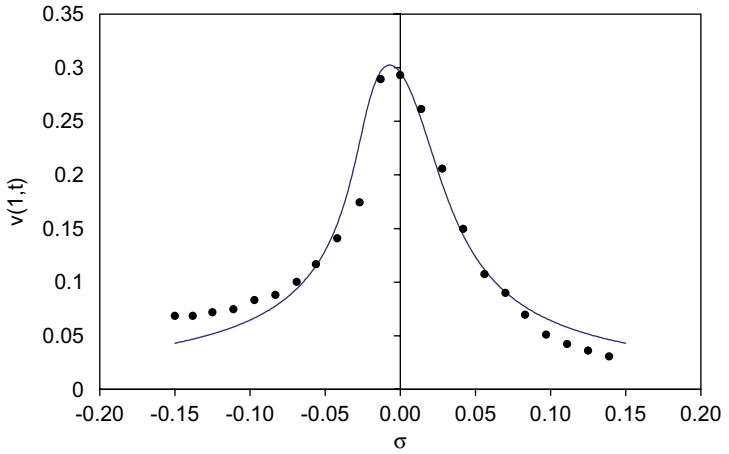

Fig. 6. First mode frequency response curve for 5% MWCNT–epoxy beam with damping ratio $\eta = 0.063$ and force $f = 0.08$ N; (–) numerical simulations and (●) experimental results.

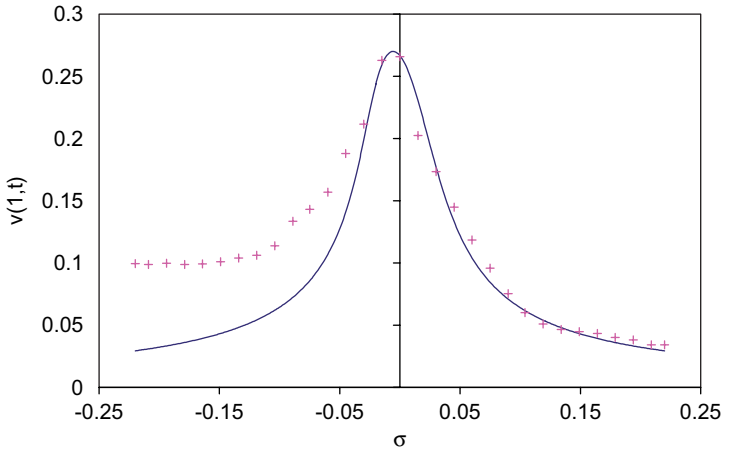

Fig. 7. First mode frequency response curve for 2.5% MWCNT–epoxy beam with damping ratio $\eta = 0.08$ and force $f = 0.08$ N; (–) numerical simulations and (+) experimental results.

response curve for 5% MWCNT–epoxy beam can be compared as plotted in Fig. 6. Considering the primary resonance condition, if $\sigma = 0$, then the excitation frequency equals to linear natural frequency $\Omega = \omega_1$. The resonance does not occur exactly in the linear natural frequency since the system is nonlinear with a nonlinear natural frequency [19].

Similarly, the comparison results between experiment and theoretical modeling for 2.5% MWCNT–epoxy beam are shown in Fig. 7. In all these results (Figs. 6 and 7), when the frequency approaches near a specific frequency (here near 20 Hz), the frequency responses change significantly due to change in sensitivity of the shaker. The inertial actuator used here has a natural frequency around 20 Hz, so the frequency response close to 20 Hz cannot be accurately obtained. The jump phenomenon is observed here in the results since the damping is strong enough and the amplitude of vibration is not too large (considering the damping) to cause the jump.

Fig. 8 shows that the increase in amplitude of excitation force causes not only the increase of the amplitude of vibration, and particularly the amplitude of resonance vibration, but also a small shift of resonance to a lower frequency. When the excitation is kept constant and the damping ratio varies as shown in Fig. 9, the amplitude of the vibration at resonance increases as the damping factor decreases. In addition, a small

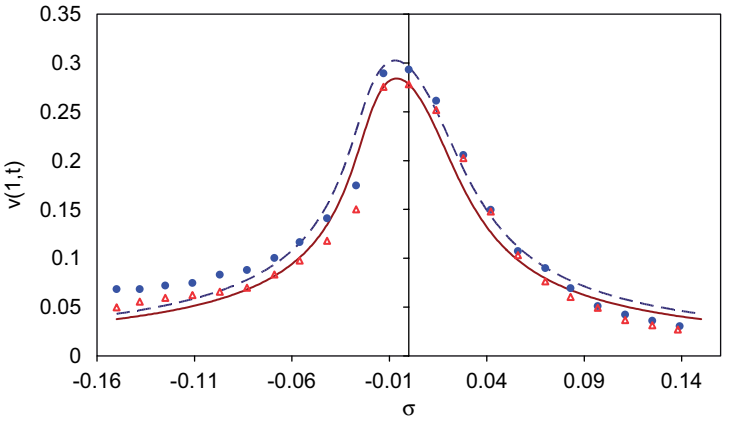

Fig. 8. Frequency response curves for 5% MWCNT–epoxy for various force with damping ratio $\eta = 0.063$; numerical simulations for $f = 0.07$ (–) and $f = 0.08$ (- -); experimental results for $f = 0.07$ N (△) and $f = 0.08$ N (●).

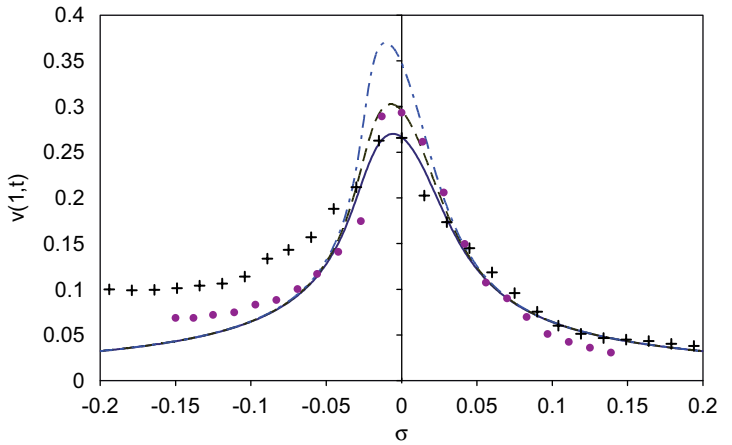

Fig. 9. Frequency response curves for various damping ratios η with force $f = 0.08$ N; (–) numerical simulations for $\eta = 0.08$, (- -) for $\eta = 0.063$ and (-•-) for $\eta = 0.04$; (+) experimental results for $\eta = 0.08$ and (●) for $\eta = 0.063$.

shift of resonance to a lower frequency appears as the value of the damping ratio reduces. The experimental data presented in Fig. 9 are for 2.5% MWCNT (i.e., $\eta = 0.063$) and 5% MWCNT (i.e., $\eta = 0.08$) to avoid undue complication in the figure. In order to provide the evaluation of the frequency response as a function of damping, the numerical results are provided for all the three samples including plain epoxy beam.

5. Conclusions

The equations of motion of planar nonlinear vibrations of an inextensible viscoelastic cantilever beam have been utilized to study the frequency response function of the system. The viscoelastic material follows a classical linear viscoelastic model, i.e., Kelvin–Voigt assumption. Using the method of multiple scales, the frequency response function and the phase-amplitude modulation equations of the system due to a direct harmonic excitation were derived for the case of primary resonance. In addition, three different sample beams were fabricated including two carbon nanotube-reinforced beams. The experimental results matched the theoretical formulations very closely. The results demonstrated that increasing the amplitude of excitation or decreasing the damping can cause a minor decrease in the nonlinear frequency of the resonance despite of an increase in amplitude of vibration due to reduced damping.

Acknowledgments and disclaimer

The materials presented here are based upon work supported in part by the National Science Foundation under CAREER Grant no. CMMI-0238987. Any opinions, findings, and conclusions or recommendations expressed in these materials are those of the authors and do not necessarily reflect the views of the National Science Foundation. The authors would also like to thank Mr. Himanshu Rajoria for his help in fabrication of the beams used here.

References

[1] S.N. Mahmoodi, S.E. Khadem, N. Jalili, Theoretical development and closed-form solution of nonlinear vibrations of a directly excited nanotube-reinforced composite cantilever beam, *Archive of Applied Mechanics* 75 (2006) 153–163.
[2] S.N. Mahmoodi, N. Jalili, S.E. Khadem, Passive nonlinear vibrations of a directly excited nanotube-reinforced composite cantilever beam, *Proceedings of 2005 ASME International Mechanical Engineering Congress & Exposition, Symposium on Vibration and Noise Control*, Orlando, FL, November 2005.
[3] T. Bailey, J.E. Hubbard Jr., Distributed piezoelectric polymer active vibration control of a cantilever beam, *AIAA Journal of Guidance Control Dynamic* 8 (1985) 605–611.
[4] Q. Wang, S.T. Quek, Flexural vibration analysis of sandwich beam coupled with piezoelectric actuator, *Smart Materials & Structures* 9 (2000) 103–109.
[5] D. Bratosin, T. Sireteanu, Hysteretic damping modeling by nonlinear Kelvin–Voigt model, *Proceeding of the Romanian Academy Series A* 3 (2002) 1–6.
[6] E. Esmailzadeh, M.A. Jalali, Nonlinear oscillations of viscoelastic rectangular plates, *Nonlinear Dynamics* 18 (1999) 311–319.
[7] H.N. Arafat, A.H. Nayfeh, C. Chin, Nonlinear nonplanar dynamics of parametrically excited cantilever beams, *Nonlinear Dynamics* 15 (1998) 31–61.
[8] M.R.M. Crespo da Silva, Nonlinear flexural–flexural–torsional–extensional dynamics of beams—I. Formulation, *International Journal of Solid Structures* 24 (1988) 1225–1234.
[9] M.R.M. Crespo da Silva, Nonlinear flexural–flexural–torsional–extensional dynamics of beams—II. Response analysis, *International Journal of Solid Structures* 24 (1988) 1235–1242.
[10] M.R.M. Crespo da Silva, Equations for nonlinear analysis of 3D motions of beams, *Applied Mechanics Reviews* 44 (1991) s51–s59.
[11] M.R.M. Crespo da Silva, C.C. Glynn, Nonlinear flexural–flexural–torsional dynamics of inextensional beams. I. Equations of motion, *Journal of Structural Mechanics* 6 (1978) 437–448.
[12] M.R.M. Crespo da Silva, C.C. Glynn, Nonlinear flexural–flexural–torsional dynamics of inextensional beams. II. Forced motions, *Journal of Structural Mechanics* 6 (1978) 449–461.
[13] N. Jalili, E. Esmailzadeh, A nonlinear double-winged adaptive neutralizer for optimum structural vibration suppression, *Journal of Communications in Nonlinear Science and Numerical Simulation* 8 (2003) 113–134.
[14] E. Esmailzadeh, N. Jalili, Parametric response of cantilever Timoshenko beams with tip mass under harmonic support motion, *International Journal of Nonlinear Mechanics* 33 (1998) 765–781.
[15] A.H. Nayfeh, C. Chin, S.A. Nayfeh, Nonlinear normal modes of a cantilever beam, *ASME Journal of Vibration and Acoustics* 117 (1995) 477–481.
[16] H.N. Arafat, A.H. Nayfeh, Investigation of subcombination internal resonances in cantilever beams, *Shock and Vibration* 5 (1998) 289–296.
[17] A.H. Nayfeh, S.A. Nayfeh, On nonlinear modes of continuous systems, *ASME Journal of Vibration and Acoustics* 116 (1994) 129–136.
[18] S.W. Shaw, C. Pierre, Normal modes of vibration for nonlinear continuous systems, *Journal of Sound and Vibration* 169 (1994) 319–347.
[19] S.N. Mahmoodi, S.E. Khadem, M. Rezaee, Analysis of nonlinear mode shapes and natural frequencies of continuous damped systems, *Journal of Sound and Vibration* 275 (2004) 283–298.
[20] J. Chung, H.H. Yoo, Dynamic analysis of a rotating cantilever beam by using the finite element method, *Journal of Sound and Vibration* 249 (2002) 147–164.
[21] S.A. Emam, A.H. Nayfeh, Nonlinear response of buckled beams to subharmonic-resonance excitations, *Nonlinear Dynamics* 35 (2004) 105–122.
[22] M. Eissa, Y.A. Amer, Vibration control of a cantilever beam subject to both external and parametric excitation, *Applied Mathematics and Computation* 152 (2004) 611–619.
[23] M.M. Kamel, Y.A. Amer, Response of parametrically excited one degree of freedom system with nonlinear damping and stiffness, *Physica Scripta* 66 (2002) 410–416.
[24] H. Rajoria, N. Jalili, Determination of strength and damping characteristics of carbon nanotube–epoxy composites, *Proceedings of 2004 ASME International Mechanical Engineering Congress & Exposition*, Anaheim, CA, November 2004.
[25] H. Rajoria, N. Jalili, Passive vibration damping enhancement using carbon nanotube–epoxy reinforced composites, *Composites Science and Technology Journal* 65 (2005) 2079–2093.

[26] P. Avouris, T. Hertel, R. Martel, T. Schmidt, H.R. Shea, R.E. Walkup, Carbon nanotubes: nanomechanics, manipulation and electronic devices, *Applied Surface Science* 141 (1999) 201–209.
[27] A.H. Nayfeh, B. Balachandran, *Applied Nonlinear Dynamics: Analytical, Computational, and Experimental Methods*, Wiley, New York, 1995.
[28] A.H. Nayfeh, *Perturbation Methods*, Wiley, New York, 1973.